# Optimal Synchronizability of Bearings

N. A. M. Araújo,[1,*] H. Seybold,[2] R. M. Baram,[3] H. J. Herrmann,[1,4] and J. S. Andrade, Jr.[4,1]

[1]*Computational Physics for Engineering Materials, IfB, ETH Zurich, Wolfgang-Pauli-Strasse 27, CH-8093 Zurich, Switzerland*
[2]*Department of Earth, Atmospheric, and Planetary Sciences, MIT, Cambridge, Massachusetts 02139, USA*
[3]*Center for Theoretical and Computational Physics, University of Lisbon, 1649-003 Lisboa, Portugal*
[4]*Departamento de Física, Universidade Federal do Ceará, 60451-970 Fortaleza, Ceará, Brazil*

(Received 10 December 2012; published 7 February 2013)

Bearings are mechanical dissipative systems that, when perturbed, relax toward a synchronized (bearing) state. Here we find that bearings can be perceived as physical realizations of complex networks of oscillators with asymmetrically weighted couplings. Accordingly, these networks can exhibit optimal synchronization properties through fine-tuning of the local interaction strength as a function of node degree [Motter, Zhou, and Kurths, Phys. Rev. E **71**, 016116 (2005)]. We show that, in analogy, the synchronizability of bearings can be maximized by counterbalancing the number of contacts and the inertia of their constituting rotor disks through the mass-radius relation, $m \sim r^{\alpha}$, with an optimal exponent $\alpha = \alpha_{\times}$ which converges to unity for a large number of rotors. Under this condition, and regardless of the presence of a long-tailed distribution of disk radii composing the mechanical system, the average participation per disk is maximized and the energy dissipation rate is homogeneously distributed among elementary rotors.

DOI: 10.1103/PhysRevLett.110.064106 PACS numbers: 05.45.Xt, 45.70.−n, 46.55.+d, 89.75.−k

A coherent synchronized motion can naturally emerge in a network of oscillators when the coupling intensity exceeds the synchronization threshold [1–4]. Synchronization is the mechanism responsible for numerous phenomena, such as, e.g., the vital contraction of cells producing the heartbeats, the harmony in an orchestra, and the coherence of an audience clapping after a performance [5–7]. However, undesired synchronization might also be responsible for neural diseases and collapse of technical infrastructures and networks [8]. Therefore, understanding how synchronization can be enhanced or mitigated is a question of paramount importance. The properties of the transition to a synchronized state are known to be a result of the interplay between the dynamics of the oscillators and the complex topology of the system [9,10]. Previous studies have shown that synchronization can be enhanced on scale-free topologies by asymmetric weighted couplings, in contrast to random graphs, where the most efficient configuration corresponds to a uniform coupling strength [11]. More precisely, by expressing the interaction strength $s_i$ of site $i$ in terms of its degree $k_i$ as $s_i \equiv k_i^{-\beta}$, where $\beta$ is a tunable parameter, Motter *et al.* [11] observed that the properties of the coupling Laplacian matrix [12] lead to optimal synchronization at $\beta = 1$. Under this condition of maximum synchronizability, the coupling strength just counterbalances the number of connections, thus minimizing the total cost associated with the network of couplings.

Space-filling bearings have been previously considered to explain the existence of seismic gaps [13], which are those regions between tectonic plates where no earthquake activity has been detected for a large period of time [14]. The idea is that the system self-organizes into a "bearing state" in which the fragments rotate without gliding friction. Systematic procedures have then been proposed to generate model bearing structures of rotors with circular and spherical shapes, in two and three dimensions, respectively, either highly symmetric [15,16] or random [17]. As depicted in Fig. 1, hierarchical space-filling packings emerge from these models in two dimensions, where the interstices among large disks are sequentially filled by smaller ones. Gliding friction is suppressed by ensuring that loops of touching disks have an even number of constituents. In this way, clockwise turning disks only touch counterclockwise rotating ones and vice versa. At steady state, the tangential velocity is the same for all contacts.

Under a different framework, hierarchically filled structures, where smaller elements (e.g, disks and spheres) are snugged into the interstices of larger ones, have been directly associated to scale-free networks [18–21]. The Apollonian packing of circles, for example, inspired the introduction of the so-called Apollonian network [18], where the sites correspond to the centers of the circles, and the edges are drawn to connect the centers (sites) of pairs of touching circles. Bearings can also be directly associated to complex networks, whose sites are given by the positions $\vec{R}_i$ of the centers of the disks. These spatial networks fulfill, for each loop of $n$ disks, the condition $\sum_{i=1}^{n-1}(\vec{R}_{i+1} - \vec{R}_i) = \vec{R}_n - \vec{R}_1$ and are scale free, if the original bearing is space filling.

One can readily identify the bearing state as a typical synchronized state. It is thus legitimate to convey that space-filling bearings rotating in steady state (i.e., when all rotors possess equal tangential velocities) are in fact physical realizations of synchronized complex networks.

 

Once this conceptual parallelism is ascertained, one can go even further and ask, in the spirit of the asymmetric coupling approach introduced in Ref. [11], whether or not such a synchronized state can be optimized through some constitutive physical property of the bearings. In what follows we show that the synchronized state of two-dimensional space-filling bearings can indeed be substantially enhanced by adequately adjusting the inertial contribution of individual rotors to the global motion of the system.

Consider a bearing of $N$ rotors. The equation of motion for the angular velocity $\vec{\omega}_i$ of rotor $i$ can be written as

$$I_i\dot{\vec{\omega}}_i = \sum_j \vec{T}_j = \sum_j r_i\vec{r}_{ij} \times \vec{F}_{ji}, \quad (1)$$

where $I_i$ and $r_i$ are the rotational inertia and radius of rotor $i$, the sum is over all rotors in contact with $i$, $\vec{F}_{ji}$ is the force of rotor $j$ on the surface of $i$, and $\vec{r}_{ij}$ is the unit vector pointing to the contact with $j$ in the reference frame of disk $i$. Taking the force $\vec{F}_{ji}$ as a dissipative force proportional to the relative velocity at the contact point, we have

$$\vec{F}_{ji} = \sigma(\vec{v}_j - \vec{v}_i) = -\sigma(\vec{\omega}_j \times r_j\vec{r}_{ij} + \vec{\omega}_i \times r_i\vec{r}_{ij}), \quad (2)$$

where $\sigma$ is the coupling between rotors and we used the identity $\vec{r}_{ji} = -\vec{r}_{ij}$. In two-dimensional bearings, since rotors are disks with fixed position (see Fig. 1), the net translational force is zero and the angular velocity can be described by a scalar. Equation (1) then simplifies to

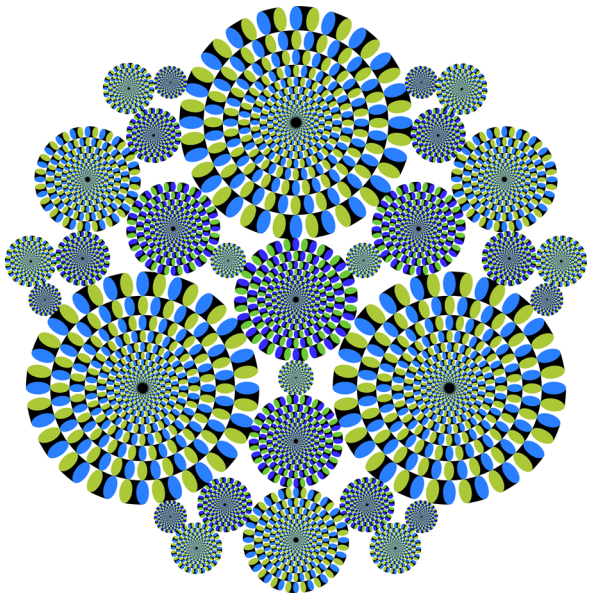

FIG. 1 (color online). Two-dimensional space-filling bearing configuration with 31 rotor disks. In order to suppress gliding friction, disks rotate either clockwise or anticlockwise, all with the same tangential velocity, and loops of touching disks always have an even number of disks. This static illusory-motion image is an adaptation from the peripheral drift illusion "Rotating Snakes" shown in Ref. [26]. Note that every two touching disks always have opposite senses of rotation.

$$I_i\dot{\omega}_i = -\sigma\sum_j A_{ij}[\omega_i r_i^2 + \omega_j r_i r_j], \quad (3)$$

where $A_{ij}$ are the elements of the connectivity matrix, defined in such a way that $A_{ij} = 1$ if two disks $i$ and $j$ are different and mutually touching and $A_{ij} = 0$ otherwise.

At this point, we introduce the following constitutive relation between the mass of disk $i$ and its radius,

$$m_i = 2ar_i^{\alpha}, \quad (4)$$

such that the rotational inertia becomes $I_i = ar_i^{\alpha+2}$, where $a = 1$ in consistent units, for convenience. It then follows that $\dot{\omega}_i = -\sigma\sum_j T_{ij}\omega_j$, where $T_{ij} = n_i r_i^{-\alpha}\delta_{ij} + r_i^{-1-\alpha} r_j A_{ij}$, $n_i$ is the number of disks touching $i$, and $\delta_{ij}$ is the Kronecker delta. In matrix form this can be written as

$$\dot{\vec{\omega}} = -\sigma\mathbf{T}\vec{\omega}, \quad (5)$$

where $\vec{\omega}$ is the $N$-dimensional vector of the angular velocities and $\mathbf{T}$ is the interaction matrix. A bearing is a dissipative system which, as already mentioned, converges to a steady state, namely the bearing state, where the tangential velocities of all rotors become equal, i.e., $v_1 = v_2 = \cdots = v_N \equiv s$, such that $\dot{s}(t) = 0$. Through the relation between tangential and angular velocities, $\vec{\omega} = \mathbf{R}^{-1}\vec{v}$, where $\mathbf{R}$ is a diagonal matrix with $R_{ii} = c_i r_i$, with $c_i = \pm 1$ depending on the sense of rotation of the disk [16], the equivalent to Eq. (5) for the $N$-dimensional vector of absolute tangential velocities $\vec{v}$ can be readily obtained, being $\dot{\vec{v}} = -\sigma\mathbf{B}\vec{v}$. The coupling matrix $\mathbf{B}$ can be written as $\mathbf{B} = \mathbf{R}\mathbf{T}\mathbf{R}^{-1}$, i.e., $B_{ij} = r_i^{-\alpha}(n_i\delta_{ij} - A_{ij})$, where we make use of $c_i/c_j = -1$ for all pairs of touching disks. In this work we focus on the relaxation after small perturbations $\vec{\xi}$ to the bearing state, namely $v_i = s + \xi_i$, which leads to the following vectorial variational equation:

$$\dot{\vec{\xi}} = -\sigma\mathbf{B}\vec{\xi}. \quad (6)$$

This system of coupled linear differential equations can be written in the space of eigenvectors of $\mathbf{B}$, $\vec{x}_k$ (with eigenvalue $\lambda_k$), such that $\vec{x}_1$ ($\lambda_1 = 0$) refers to perturbations along the stable manifold of the bearing state. All other eigenvectors are transverse to $\vec{x}_1$ [12]. Due to the linear nature of Eq. (6), the Lyapunov exponents correspond to $-\sigma\lambda_k$. Since all eigenvalues are non-negative in this problem (the matrix $\mathbf{B}$ can be symmetrized), the stability of the bearing state is guaranteed [22]. In analogy to the work of Motter *et al.* [11], the factors $r_i^{-\alpha}$ present in the elements of $\mathbf{B}$ correspond to the weights of the pairwise interactions. As we show next, in the complex network associated with the topology of the bearings, the number of contacts is an increasing function of the radius and so it becomes possible to enhance synchronization by tuning the coupling weights in such a way as to balance the number of contacts.

Perturbations along the bearing states ($\dot{\vec{\xi}} = 0$) lead the system from one bearing state to another with a different

tangential velocity $s$; i.e., all tangential velocities change by the same amount, regardless of the value of $\alpha$ ($\xi_i \equiv \xi$). These perturbations are related to the eigenvalue $\lambda_1 = 0$. Hereafter, we focus on perturbations that are transverse to the bearing states, i.e., perturbations after which the system always relaxes back to the original bearing state. Specifically, the objective is to investigate the dependence on the inertial parameter $\alpha$ of the smallest (nonzero), $\lambda_2$, and largest, $\lambda_N$, eigenvalues of the system described by the matrix **B**. These eigenvalues correspond to the slowest and fastest relaxation modes, respectively. Generally speaking, for perturbations out of the bearing manifold ($\lambda \neq 0$), the larger the eigenvalues the faster the relaxation toward the stable state. Here two features come into play: the mass (inertia) distribution of the disks and the number of contacts. While the former depends explicitly on $\alpha$, the latter is an increasing function of the rotor radius. Numerical results for a bearing (of type $n = m = 0$ of the first family for loops of size 4 [15]) with 4511821 disks reveal that the average number of contacts scales with the disk radius as $r^{\gamma}$, with $\gamma = 0.94 \pm 0.04$, which should approach unity in the limit of space filling systems.

As depicted in Figs. 2(a) and 2(b) $\lambda_2$ and $\lambda_N$ generally increase with $\alpha$, although changes in the behavior of both eigenvalues can be observed at a crossover value $\alpha_\times \approx 1$. While $\lambda_N$ increases faster for $\alpha > \alpha_\times$, the increase of $\lambda_2$ becomes attenuated in the same range of $\alpha$ values. The insets of Figs. 2(a) and 2(b) show that, for $\alpha > \alpha_\times$, $\lambda_2$ and $\lambda_N$ are increasing functions of the number of disks, since the ones with higher inertia also possess more contacts to shed any perturbation. The same description applies for all eigenvalues. For $\alpha < \alpha_\times$, the inertia assigned to each disk does not always compensate its number of contacts. For example, the fact that $\lambda_2$ decreases with $N$ for $\alpha = -1$ reflects this imbalance. More general conclusions can be drawn from the eigenratio between the largest and smallest (nonzero) eigenvalues of the coupling matrix, $\lambda_N/\lambda_2$ [12,23]. This ratio solely depends on geometrical features (radii, network topology, and disk mass) and not on the initial conditions for the velocities. The lower the ratio, the higher the synchronizability [12,23]. As shown in Fig. 2(c), bearings consisting of rotors with masses that follow the relation, $m \sim r^{\alpha_\times}$, have a minimum eigenratio value, in analogy to the optimal synchronization coupling found for scale-free networks [11]. Interestingly, the larger the value of $N$, the more sensitive is the system to variations of $\alpha$. Moreover, the results in the inset indicate that regardless of the value of $\alpha$, the eigenratio increases monotonically with the number of disks. Nevertheless, since this increase is less pronounced for $\alpha = 1$ than for any other value of $\alpha$, the relative depth of the minimum augments with system size. As a consequence, large systems display an enhanced relative synchronizability at $\alpha = \alpha_\times$. In the Supplemental Material [24] we show the convergence of $\alpha_\times$ towards unity in the thermodynamic limit.

To shed light on the dependence on $\alpha$ of the contribution of disks to the eigenmodes, we define the average participation [25] as

$$P = \frac{1}{N} \sum_{\vec{x}_k} \frac{[\sum_{j=1} \vec{x}_k(j)^2]^2}{\sum_{j=1} \vec{x}_k(j)^4}, \tag{7}$$

where the outer sum is over all eigenvectors $\vec{x}_k$ and the inner sums are over the components of the eigenvector. As shown in Fig. 3, there is an intermediate range of $\alpha$ values, for a given system size $N$, where an enhanced average participation per disk can be clearly observed. However, our results suggest that the value of $\alpha$ for which the participation becomes maximum increases in a discontinuous fashion from $\alpha \approx 0.5$ to 1.0, as the system size increases from $N = 613$ to 31531. The inset of Fig. 3 shows that, notwithstanding the value of $\alpha$, the average participation per disk decreases with the number of disks $N$, but with a slope that is milder for $\alpha = 1.0$ than for any other case. This behavior expresses the more homogeneous contribution of rotors to the system dynamics. In this range of $\alpha$ values, the number of contacts of each disk is approximately compensated by its inertia. Accordingly,

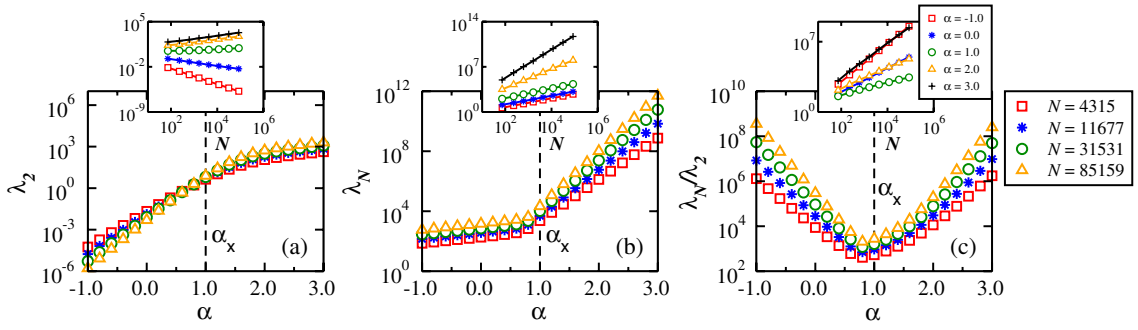


FIG. 2 (color online). Dependence on the exponent $\alpha$ of the lowest (nonzero) $\lambda_2$ (a) and the largest $\lambda_N$ (b) eigenvalues of the matrix **B**. The same is shown in (c), but for the ratio $\lambda_N/\lambda_2$. The insets show the system size dependence for different values of $\alpha$. Both $\lambda_2$ and $\lambda_N$ increase with $\alpha$ exhibiting a change in the behavior at the crossover value $\alpha_\times$ (dashed lines): the faster increase of $\lambda_2$ is for $\alpha < \alpha_\times$, while $\lambda_N$ grows faster for $\alpha > \alpha_\times$. As a consequence, a minimum is observed for the ratio $\lambda_N/\lambda_2$ at the crossover value $\alpha_\times$.

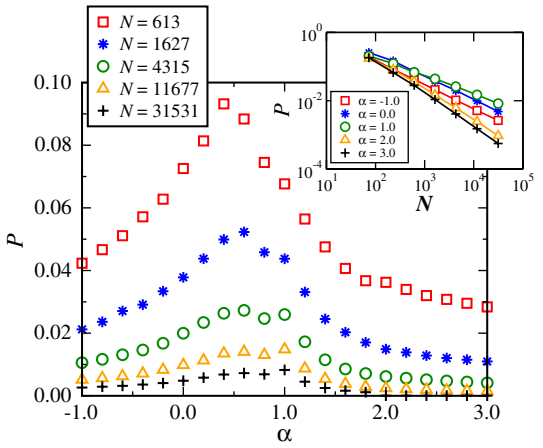


FIG. 3 (color online). $\alpha$ dependence of the average participation $P$ for bearings with different number of disks. An enhanced participation per disk is observed for an intermediate range of $\alpha$. Results suggest a discontinuous change in the position of the maximum as discussed in the text. In the inset, the size dependence is included for different values of $\alpha$. The participation per disk decreases with the number of disks with the smallest slope for $\alpha = 1.0$.

we expect $\alpha_\times$ to converge toward $\gamma \approx 1.0$ as the number of disks increases. Under these conditions, the impact of changes in the tangential velocity of a disk becomes relatively less dependent on its radius.

It is also interesting to calculate the rate at which energy is dissipated. For rotor $i$, we have $W_i = I_i v_i \dot{v}_i / r_i^2$. Now, given an eigenmode $k$ with eigenvalue $\lambda_k$, the velocity of disk $i$ can be expressed by the $i$th component of $\vec{x}_k(i)$ scaled by a constant $c$, i.e., $v_i = c\vec{x}_k(i)$. Thus, one obtains the relation $\dot{v}_i = -c\lambda_k \sigma \vec{x}_k(i)$. Based on this result, we can decompose the dissipation rate of disk $i$ in its different modes, $W_{ki} = -r_i^\alpha c^2 \lambda_k \sigma \vec{x}_k(i)^2$. It is then possible to quantify how dissipation is distributed among disks, by defining the relative dissipation of disk $i$ in the eigenmode $k$ as $Q_i^k = W_{ki}/\sum_j W_{kj}$, which leads to

$$Q_i^k = \frac{r_i^\alpha \vec{x}_k(i)^2}{\sum_j r_j^\alpha \vec{x}_k(j)^2}. \tag{8}$$

Figure 4 shows, for different values of $\alpha$, the dependence on the radius $r$ of the relative dissipation rate of a rotor $i$ averaged over all eigenmodes, $Q_i = 1/M \sum_k Q_i^k$, where $M$ is the total number of eigenmodes. For $\alpha < 1.0$, the dissipation is an increasing function of $r$, while for $\alpha > 1.0$, larger disks dissipate less energy than smaller ones. By tuning $\alpha = 1.0$, the dissipation rate becomes more uniformly distributed among all disks, being approximately invariant on the rotor size. Figure 5 consists of snapshots for three different values of $\alpha$, showing how the average dissipation rate is typically distributed among disks in a bearing with 613 disks.

In summary, we have shown that bearings are physical realizations of complex networks of oscillators. When the bearings consist of rotors of different sizes, the coupling between oscillators is asymmetric, as the effect of a pairwise interaction on the rotors motion depends on their inertia (typically different for each one). Once this parallelism is established, it is possible to evaluate the stability of these mechanical systems applying concepts from dynamic systems theory. In particular, our results for two-dimensional space-filling bearings, characterized by a scale-free distribution of rotor (disk) contacts, indicate that their synchronizability can be duly maximized. This is achieved by counterbalancing the number of contacts of the disks with their inertia through the mass-radius relation, $m \sim r^{\alpha_\times}$, where $\alpha_\times$ is the optimal exponent which we expect to asymptotically converge to unity as the number of rotors increases. Under this condition, in spite of the power-law distribution of radii, the average participation per disk has a maximum and the energy dissipation rate is homogeneously distributed among disks.

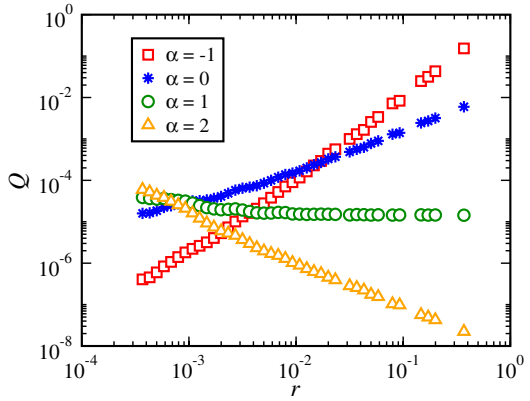


FIG. 4 (color online). Radius dependence of the relative dissipation rate $Q$ of each disk for different values of $\alpha$, obtained for a bearing of 85159 disks. While for $\alpha < 1.0$, $Q$ is an increasing function of the disk radius $r$, for $\alpha > 1.0$ larger disks dissipate less energy as the number of contacts does not compensate the increase in disk inertia.

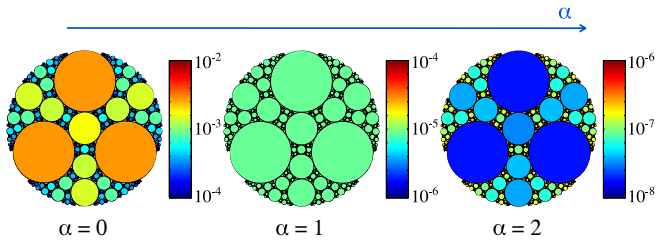


FIG. 5 (color online). Snapshots of bearings with 613 disks and different values of $\alpha$. The color stands for the average dissipation rate $Q$ in a logarithmic scale. For $\alpha \neq 1$, $Q$ strongly depends on the radius of the disk (color depends on the radius). While for $\alpha < 1$ the dissipation rate is an increasing function of the radius, for $\alpha > 1$ is a decreasing function. For $\alpha = 1$ the dissipation rate is of the same order of magnitude to every disk (same color).

We thank Heitor Credidio for help in the preparation of Fig. 1. We acknowledge financial support from the European Research Council (ERC) Advanced Grant No. 319968-FlowCCS, the Brazilian Agencies CNPq, CAPES, FUNCAP, and FINEP, the FUNCAP/CNPq Pronex grant, and the National Institute of Science and Technology for Complex Systems in Brazil.

*nuno@ethz.ch

[1] A. Pikovsky, M. Rosenblum, and J. Kurths, *Synchronization: A Universal Concept in Nonlinear Sciences*, Cambridge Nonlinear Science Series Vol. 12 (Cambridge University Press, Cambridge, England, 2003).

[2] J. A. Acebrón, L. L. Bonilla, C. J. P. Vicente, F. Ritort, and R. Spigler, Rev. Mod. Phys. **77**, 137 (2005).

[3] G. Osipov, J. Kurths, and C. Zhou, *Synchronization in Oscillatory Networks* (Springer Verlag, Berlin, 2007).

[4] S. Boccaletti, *The Synchronized Dynamics of Complex Systems* (Elsevier, New York, 2008).

[5] Z. Néda, E. Ravasz, T. Vicsek, Y. Brechet, and A. L. Barabási, Phys. Rev. E **61**, 6987 (2000).

[6] A. T. Winfree, Science **298**, 2336 (2002).

[7] S. H. Strogatz, *Sync: the Emerging science of spontaneous order* (Hyperion, New York, 2003).

[8] S. Strogatz, D. Abrams, A. McRobie, B. Eckhardt, and E. Ott, Nature (London) **438**, 43 (2005); S. Floyd and V. Jacobson, IEEE/ACM Trans. Netw. **1**, 397 (1993); L. Glass, Nature (London) **410**, 277 (2001); V. H. P. Louzada, N. A. M. Araújo, J. S. Andrade Jr., and H. J. Herrmann, Sci. Rep. **2**, 658 (2012).

[9] S. Assenza, R. Gutiérrez, J. Gómez-Gardeñes, V. Latora, and S. Boccaletti, Sci. Rep. **1**, 99 (2011).

[10] J. Gómez-Gardeñes, S. Gómez, A. Arenas, and Y. Moreno, Phys. Rev. Lett. **106**, 128701 (2011).

[11] A. E. Motter, C. Zhou, and J. Kurths, Phys. Rev. E **71**, 016116 (2005); A. E. Motter, C. S. Zhou, and J. Kurths, Europhys. Lett. **69**, 334 (2005).

[12] J. F. Heagy, L. M. Pecora, and T. L. Carroll, Phys. Rev. Lett. **74**, 4185 (1995); L. M. Pecora and T. L. Carroll, Phys. Rev. Lett. **80**, 2109 (1998).

[13] S. Roux, A. Hansen, H. J. Herrmann, and J.-P. Vilotte, Geophys. Res. Lett. **20**, 1499 (1993).

[14] C. Lomnitz, Bull. Seismol. Soc. Am. **72**, 1411 (1982).

[15] H. J. Herrmann, G. Mantica, and D. Bessis, Phys. Rev. Lett. **65**, 3223 (1990).

[16] R. MahmoodiBaram, H. J. Herrmann, and N. Rivier, Phys. Rev. Lett. **92**, 044301 (2004).

[17] R. MahmoodiBaram and H. J. Herrmann, Phys. Rev. Lett. **95**, 224303 (2005).

[18] J. S. Andrade Jr., H. J. Herrmann, R. F. S. Andrade, and L. R. da Silva, Phys. Rev. Lett. **94**, 018702 (2005).

[19] F. Varrato and G. Foffi, Mol. Phys. **109**, 2663 (2011).

[20] S. D. S. Reis, N. A. M. Araújo, J. S. Andrade Jr., and H. J. Herrmann, Europhys. Lett. **97**, 18 004 (2012).

[21] Z. Zhang, J. Guan, W. Xie, and S. Zhou, Europhys. Lett. **86**, 10 006 (2009); C. N. Kaplan, M. Hinczewski, and A. N. Berker, Phys. Rev. E **79**, 061120 (2009); A. Halu, A. Vezzani, and G. Bianconi, Europhys. Lett. **99**, 18 001 (2012).

[22] D. W. Jordan and P. Smith, *Nonlinear Ordinary Differential Equations* (Oxford University Press, New York, 2007), 4th ed.

[23] M. Barahona and L. M. Pecora, Phys. Rev. Lett. **89**, 054101 (2002).

[24] See Supplemental Material at http://link.aps.org/supplemental/10.1103/PhysRevLett.110.064106 for the convergence of the exponent $\alpha_\times$ with system size $N$.

[25] B. Kramer and A. MacKinnon, Rep. Prog. Phys. **56**, 1469 (1993); R. J. Bell and P. Dean, Discuss. Faraday Soc. **50**, 55 (1970); P. A. Morais, J. S. Andrade Jr., E. M. Nascimento, and M. L. Lyra, Phys. Rev. E **84**, 041110 (2011).

[26] I. Kuriki, H. Ashida, I. Murakami, and A. Kitaoka, J. Vis. **8**, 16 (2008); http://www.ritsumei.ac.jp/~akitaoka/index-e.html, Akiyoshi's illusion pages (accessed in November 2012).